Title
SECONDARY ELECTRON DISTRIBUTION FOR HEAVY IONS

Authors
Oda, Nobuo
Lyman, John T.

Publication Date
1965-09-15

UCRL-16405 Rev.

University of California

Ernest O. Lawrence Radiation Laboratory

SECONDARY-ELECTRON DISTRIBUTION FOR HEAVY IONS

Berkeley, California

To be published in
Radiation Research supplement

UCRL-16405 Rev.
Preprint

UNIVERSITY OF CALIFORNIA

Lawrence Radiation Laboratory
Berkeley, California

AEC Contract No. W-7405-eng-48

SECONDARY-ELECTRON DISTRIBUTION FOR HEAVY IONS

Nobuo Oda and John T. Lyman

September 1966

SECONDARY-ELECTRON DISTRIBUTION FOR HEAVY IONS

Nobuo Oda* and John T. Lyman

Lawrence Radiation Laboratory
University of California
Berkeley, California

September 1966

I. INTRODUCTION

The specification of transverse distribution of energy deposition along the track of a fast charged particle is of basic importance in understanding the effects of heavy ions in passing through matter. The transverse distribution results from absorption of energy by the medium due primarily to the slowing down of the secondary electrons which have been ejected from the primary particle's track.

Delta (δ) rays are generally those secondary electrons that have an initial energy above some arbitrary threshold value so that there is a high probability that most of their energy will not be deposited in the vicinity of the ion track. An alternative definition would be that δ rays are all secondary electrons which are ejected further than a given arbitrary distance from the ion track.

In radiation biology, many radiation effects of heavy ions have been interpreted in terms of an inactivation cross section. Part of this total cross section is due to the ion track and another part is due to δ rays. The estimated cross section due to the δ rays is subtracted from the total cross section to obtain the cross section due to the ion track. This procedure is called the δ-ray correction.

*Present address: Tokyo Institute of Technology, Meguro-Ku, Tokyo.

Although it is well-known that the contribution of δ rays to the radiation effect of heavy ions is quite significant, our knowledge of δ rays is very poor experimentally as well as theoretically. Thus far, almost all the δ-ray corrections have been made with several simplified assumptions about the processes of δ-ray production as well as on their slowing down, which have not yet been verified by experiment. Although it is most desirable to obtain complete experimental knowledge of the physical properties of the δ rays, some specific information on δ rays may suffice (depending on the methods of interpretation of the radiation effects, such as the target-theoretical analysis) for the study of the biological effect. Therefore, first let us discuss two alternative possible approaches to the δ-ray correction in connection with the present status of experimental information available for the low-energy secondary electrons. Then we will present results of the measurements carried out on the secondary electrons from heavy ions from the Lawrence Radiation Laboratory's Hilac. Finally we will discuss the implication of the above results to several related problems.

II. TARGET THEORY AND DELTA-RAY CORRECTION

The two alternative approaches are the "space-averaged picture" and the "extended-track picture."

A. Space-Averaged Picture

The exact formulation of this approach was first given by Lea (1). Lea derived the δ-ray correction in terms of the "associated volume," in which the so-called overlapping factor F was calculated on the assumption of a "one-ionization model." A similar approach has been applied by Dolphin and Hutchinson (2) to heavy-ion irradiation of enzymes. We call this method "space-averaged picture" because it does not take into account the spatial correlation between δ-ray tracks and the primary track, but regards δ rays as distributed uniformly in space, with the intercorrelation among ions along the same δ-ray track considered as taken into account through the overlapping factor, F. A reformulated form of this approach may be given (3) as (i) derivation of the slowing-down spectrum of δ rays, $\phi_\delta(E)$, from the primary particle flux $\phi_p(E)$; (ii) derivation of the inactivation cross section (or volume) with the use of the total differential flux, $\phi_t = \phi_p(E) + \phi_\delta(E)$, following the calculation method given in reference 3. This space-averaged picture is expected to be a good approximation for a target that is small compared with the average δ-ray range. The most important quantity in this picture is naturally the slowing-down spectrum of the δ rays, $\phi_\delta(E)$, which can be theoretically derived with the use of the information on the production of secondary electrons by the primary particles and the slowing down process of secondary electrons.

a. The production of secondary electrons by the primary particles is described in terms of the emission cross section $d\sigma(E)$ for the production of secondary electrons with energies between E and E + dE per unit primary-particle flux. These cross sections are usually obtained from the Rutherford formula which applies to knock-on collision, but for low-energy secondary electrons with well below, say, several hundred electron volts, some deviation from that formula would be expected. Therefore, the cross section for the production of low-energy secondary electrons must be determined experimentally. This kind of experiment has been carried out for 50- to 150-keV protons (4), but the experimental data do not cover the whole range of energy as well as the ion species usually used in the radiation-biological experiments with heavy ions.

b. The slowing-down process of secondary electrons requires information on the collision cross section of electrons over the energy range from the maximum δ-ray energy down to nearly zero energy for the biologically important elements. Theoretical calculations have been performed, so far, with the use of the theoretical formulae for the stopping power (Bethe-Bloch formula) and for the collision cross section (Møller formula) by Spencer and Fano (5). However, this slowing-down theory has been experimentally examined only at energies above about 50 keV (6), and its validity well below this energy is still not established.

Unfortunately, the maximum energy of δ rays for heavy ions with energy 10 MeV/amu (extensively used for radiobiological experiments with the Hilac) is about 20 keV. This implies that there is now no experimentally verified slowing-down theory available for the slowing-down spectrum associated with heavy-ion beams produced by the Hilac.

For electron energies below about 10 keV, the cross section for inelastic collisions depends critically on the electron energy because of the varying participation of inner-shell electrons in the collision process.

A number of measurements at energies below 10 keV have been made for studies of electrons backscattered from solids (7, 8) as well as of the transmission of electrons through thin foils (9). From these measurements, some important information can be derived for electron energies from 1 to 10 keV. Three useful pieces of information are (1) the range-energy relations shows no significant dependence on the atomic number of material when the range is measured in mass per unit area; (2) the scattering process is predominantly inelastic; and (3) an estimate of the mean free path for inelastic collisions is in good agreement with the prediction of the Bohr-Bethe theory when the inner-shell effect is taken into account. We can us such information to derive the slowing-down spectrum for the energy range down to 1 keV.

One may expect that extensive modification of the theory will be necessary before it is valid for electron slowing-down at energies of the order of the K-shell binding energy or less. (The electron slowing-down spectrum has not yet been directly measured at these low energies.) At the same time, it is readily understood that experimental study of such quantities as the emission cross section of secondary electrons with heavy ions and the collision cross section as well as the stopping power of low-energy electrons is required before any working theory of the electron slowing-down in the low-energy region can be established.

B. Extended-Track Picture

In this picture, the fundamental quantities may be the differential flux of secondary electrons, expressed as $\phi_\delta(E, r)$, where r is the distance from the track of the primary particle, or the energy flux per unit surface, $D(r)$, out of the cylinder of radius r. The cylinder is cooaxial with the primary particle track. Unfortunately, there is little relevant experimental data on either of the above quantities.

The quantity $D(r)$ can be derived in principle from a knowledge of $\phi_\delta(E, r)$; it can also be derived approximately from the combination of the cross section for emission of secondary electrons by heavy ions and the energy-dissipation distribution expressed as a function of distance from the secondary-electron source. The latter was calculated by Spencer (10) for the primary-electron energies above 25 keV for media of low atomic number. For energies below 25 keV the Spencer theory cannot be expected to be valid and another treatment might be useful, such as the utilization of the range-energy curve for electrons.

This picture properly takes into account the high concentration of activation events in the vicinity of the primary track and also strongly relates to the "track" model of water radiolysis (11). This "track" model, based on the diffusion kinetics of radicals, and taking account of the effects of the distribution of spur sizes and δ-ray tracks, has been fairly successful in explaining molecular yield effects (12). The "track" model is a kind of indirect-action model in terms of radiation biology, and along these lines we shall be able to construct an indirect-action theory of biological action, as an extension of the pioneer work by Zirkle and Tobias (13).

Along the latter line, Deering and Hutchinson (14) have made some calculations on $D(r)$, based on several assumptions on the production of secondary electrons, the range-energy relation, and the overall rate of energy deposition of an electron at a distance r from the primary ion track. We will not discuss the details of the δ-ray correction for the extended-track picture in this discussion.

III. LOW-ENERGY SECONDARY-ELECTRON FLUX PRODUCED BY HIGH-ENERGY HEAVY IONS

Even if the slowing-down spectrum of secondary electrons were obtained by theoretical calculations with the use of the stopping-power information derived from the experiments discussed in Section IIAb, such a spectrum would not cover the energy range below about 1 keV. At this time, to obtain the spectrum below 1 keV, we must rely on the direct measurement of the slowing-down spectrum from heavy ions.

As a first step in measuring the low-energy secondary-electron flux from heavy ions, an experiment has been done with the Hilac to measure the absolute yield and the slowing-down spectrum of secondary electrons with energies below 50 eV. This experiment is the direct measurement of $\phi_\delta(E)$, described in Section IIA, which is the differential flux of secondary electrons at a point in a medium bombarded with heavy ions. Some of the results are discussed here.

The apparatus is shown in Fig. 1, where the target consists of three foils, each of which has a thickness approximately equal to the range of the maximum-energy δ rays. The primary energy of heavy ions was varied with the use of aluminum absorber wheels, and the primary beam intensity was measured by a Faraday cup. A negative voltage (-1200 V) was applied on the suppressor ring between the target and the Faraday cup to prevent disturbance of the reading of the primary beam on the Faraday cup by exchange of secondary electrons produced both from the rear surface of the target and from the Faraday cup. We carried out these measurements at a vacuum of the order of 10^{-8} torr, to keep the target surface clean during the measurements.

The method of measurement, the same as that used by Shatas et al. (15), is indicated schematically in Fig. 2. The heavy-ion beam from Hilac passes through the sandwich arrangement consisting of three foils and then is stopped by the Faraday cage. The yield from the upstream face of target 2 can be determined from the observation of the current $I_T(V_1)$ corresponding to two alternative sets of electrode potentials. Thus, if target 3 is maintained at an arbitrary constant voltage V_3, the measured target current I_T is given by

$$I_T(V_1 < 0) = I_{21}(>V_1) - I_{12} + I_{2D} \qquad (1)$$

$$I_T(V_1 = 0) = I_{21} - I_{12} + I_{2D} \qquad (2)$$

where $I_{21}(>V_1)$ represents the current of secondary electrons leaving target 2 from the upstream surface with a normal velocity component sufficient to overcome the retarding potential V_1, and I_{12} is the current of secondary electrons reaching target 2 from target 1. Since V_2 is unchanged, the contribution to I_T by electrons flowing to or from the downstream face of target 2 is constant and is represented by I_{2D}. Equation (2) means that when the potential difference between target 1 and target 2 is zero, all secondaries from each target reach the other. The net current of secondary electrons leaving target 2 from the upstream surface with energies sufficient to overcome the retarding potential V_1, is obtained by subtracting Eq. (1) from Eq. (2). The yield from the downstream face of target 1 can also be deduced from the measurements of $I_T(V_1 > 0)$ by invoking the corresponding relationships

$$I_T(V_1 > 0) = -I_{12}(>V_1) - I_{12} + I_{2D}. \qquad (3)$$

The composite yield, i.e. the sum of yields from two opposite surfaces, is given by

$$\delta = [I_T(V_1 > 0) - I_T(V_1 < 0)]/N_p \qquad (4)$$

where N_p is the number of primary heavy particles passing through the targets and is deduced from the measurements of current I_p on the Faraday cage and information of the effective charge of the heavy ions entering the Faraday cage. Following the convention in the so-called "secondary emission," we chose $|V_1| = 45$ V to derive the yield. Actually, the yields were constant at $|V_1| > 45$ V within an experimental error. The yield, δ, defined by Eq. (4) can be related to the flux of the slowing-down spectrum $\phi_\delta(E)$, or the number of electrons per unit area per unit energy interval per unit primary heavy-particle flux by

$$\delta = \int_0^{45\ \mathrm{eV}} \phi_\delta(E)dE/\phi_H, \qquad (5)$$

where ϕ_H is the primary heavy-particle flux.

The derivation of Eq. (1) is based on the assumption that the number of secondary electrons with energies above 45 eV is negligibly small compared with that of energies below 45 eV, and this assumption was very valid in this experiment. Since the flux, $\phi_\delta(E)$, can be defined at an arbitrary point in a space between target 1 and target 2 by using relation (2), the measurements on δ can give information on the secondary electron flux in the medium.

The energy spectra of secondary electrons were obtained by the same procedure as that used to obtain the yields, except V_1 was varied from -45 V to +45 V in successive small increments, following the method described by Schultz and Pomerantz (16). In order to derive the energy spectrum from the measurements with the sandwich-target arrangement, the angular distribution of secondary electrons has to be assumed, and two kinds of angular distributions were assumed, isotropic and cosine. The energy spectra for Al with He ions of two different velocities are shown in Figs. 3 and 4.

It is interesting to see that the energy spectrum is almost insensitive to the assumed angular distribution as well as to the primary energy. The energies, the stopping powers (dE/dx), and the effective charges (Z_{eff}) of the primary heavy ions at several points, e.g., between targets 1 and 2, and a point in the front of the Faraday cage, were derived from the data of Northcliffe (17) and Roll and Steigert (18).

In Fig. 5 the yields are plotted as a function of Z^2_{eff} for various ions and a Ni target. Note that the yields for various ions with the same velocity (8.5 MeV/amu) lie on the straight line passing through the origin, and the yields for an ion of different velocity (8.8 MeV/amu oxygen) deviate from that line. This fact seems to imply that the yield is proportional to the dE/dx of the primary ions, because the dE/dx is proportional to Z^2_{eff}. However, that this is in general not the case is shown in Fig. 6, where the yields are plotted as a function of dE/dx. From Fig. 6 it is easily seen that yields with different velocities for each kind of ion are not proportional to the corresponding values of dE/dx. For each kind of ion, the higher-velocity primary particle has the higher specific yield (yield per unit energy absorption).

The following results are obtained from the data:

(i) When the velocities of primary ions are the same, the yields for each kind of ion are proportional to the dE/dx for that ion (see Fig. 5). (ii) When the velocities are different for each kind of ion, the specific yield for higher velocity is higher than that for lower velocity (see Fig. 6). These results seem to be strongly related to the production of high-energy secondary electrons by the primary particles, because the maximum energy of δ rays is proportional to the energy of the primary particles. It may be surprising that the low-energy part of the slowing-down spectra of δ rays shows a strong dependence on the maximum energy of δ rays.

IV. EFFECTS OF LOW-ENERGY SECONDARY ELECTRONS

Although the role played by low-energy secondary electrons in biological effects has not been investigated much so far, several related problems have received considerable attention in recent years. Several examples are presented in the following, which would suggest the importance of studying the behavior of the low-energy part of secondary-electron flux.

A. Triplet (Metastable)-State Excitation

In photochemistry, it is well-known that triplet metastable-state excitations can play an important role, such as the sensitized fluorescence in a mixed gas through a collision of the second kind. An example is the enhancement effect of added gases on the sensitized fluorescence of thallium atoms in mercury vapor activated by the mercury resonance radiation at 2537 Å. In this case the metastable 6^3P_0 mercury atoms are produced through the second-kind collision between the 6^3P_1 mercury atoms originally produced by the absorption of 2537 A line and the added gases (argon or nitrogen). The 6^3P_0 metastable state atoms have a long mean life and apparently can survive many collisions with argon atoms or nitrogen molecules without losing their activation. Therefore, they can remain activated until they collide with a thallium atom.

A similar process occurs when the addition of nitrogen to a mixture of hydrogen and mercury vapor increases the rate of reaction between hydrogen and metallic oxides through the formation of 6^3P_0 mercury atoms (19).

The excitation of optically forbidden spin states by electron impact is a resonant process, so that only electrons with energies close to the excitation energy are effective in this process (20, 21). The method of producing the metastable state of the atom by low-energy electron impact has been recently used for Ne with good efficiency (22).

Whether production of the metastable states by the low-energy component of the slowing-down spectrum of δ rays plays an important role is an interesting problem and should demand attention. Platzman's observations (23) that the superexcited-state excitations play a more important role in the radiation chemistry of gases than the lower-state excitations is very important in this connection, and more extensive experimental work on the role of metastable states in radiation effects is highly desired to answer such questions.

B. Subexcitation Electrons

The important role played by the subexcitation electrons for the total ionic yield in the gas and the yield of F centers in ionic crystals, in both of which some admixed contaminants play a significant role, has been pointed out by Platzman (24, 25). Thus, for the cases in which minor components experience major effects, the usually accepted statement--that the primary absorption of energy from ionizing radiation by different components of a system is in approximate proportion to their molecular concentrations--may be grossly erroneous. For biological molecules, it is highly possible that the role of the lower-energy electrons may not be minor, because the crucial molecular bonds for the radiation effects may in a sense be regarded as minor components. Further, it is to be noted that, for gases, 15 to 20% of the absorbed energy comes from the subexcitation electrons, in the case of high-energy radiations.

C. Cavity Ionization Chamber (Greening Effect)

It is well known that a cavity ionization chamber shows the polarity effect when used at very low gas pressure. This phenomenon has been explained by Greening (26) to be due to the low-energy electrons emerging from the walls of an irradiated chamber, and is called the Greening effect. This effect restricts the exact applicability of the cavity principle which is supposed to be exactly valid at the limit of low gas pressure. This should have some bearing on the dosimetry of heavy ions when the cavity chamber is used, but no experimental work has been done on this yet.

D. Fluorescent Response of a Scintillation Crystal to Heavy Ions

The fluorescence of a scintillation crystal caused by ionizing radiation is a type of radiation effect, and has been studied by many people. Results obtained by Newman et al. (27, 28) with heavy ions are very interesting from the viewpoint used in this paper. The specific fluorescence (dL/dx) of a NaI(Tl) crystal is shown as a function of dE/dx in Fig. 7.

It is very interesting to note that the specific fluorescence is not a function of dE/dx alone, but is instead a function of the velocity of the primary heavy ions, just as is the yield curve of the low-energy secondary electrons shown in Fig. 5. It is probable that this similarity might show some fundamental interrelation between the fluorescence effect and the low-energy electron flux. Meyer and Murray (29) gave a theoretical interpretation of this phenomenon based on the extended-track picture (Section IIA). However, since the fluorescence effect is one of the phenomena in which a minor component (i.e., fluorescent center) plays a major role, the low-energy electron flux might significantly contribute to that effect.

In a sense the specific fluorescence corresponds to the inactivation cross section in radiation biology; much more experimental work should be done in radiation biology, too, with heavy ions with different energies, to elucidate the mechanism of the δ-ray effects. The above discussion will have some bearing on the problem of the definition of radiation quality for heavy ions, in connection with radiation effects as well as dosimetry.

SUMMARY

Two kinds of approaches to the δ-ray correction for heavy ions are discussed: "space-averaged picture" and "extended-track picture." The fundamental quantity for the "space-averaged picture" is the differential flux (slowing-down spectrum) $\phi_\delta(E)$ of δ rays. Experimental results are presented on the energy spectra and absolute yield values of the low-energy part of $\phi_\delta(E)$. The most interesting results are as follows:

(i) When the velocities of primary ions are the same, the yields for each kind of ion are proportional to dE/dx.

(ii) When the velocities are different for each kind of ion, the specific yield for higher velocity is higher than that for lower velocity. The discussion of several related problems suggests the importance of studies on the behavior of energy spectra of the secondary-electron flux.

ACKNOWLEDGMENTS

The authors are much indebted to Dr. C. A. Tobias, whose interest made this work possible, and to Jerry Howard and David Love, for their excellent technical assistance. We also wish to thank Dr. E. Newman and Dr. F. E. Steigert for permission to use their graph (Fig. 7) of the specific fluorescence of a NaI(Tl) crystal.

This work was supported jointly by the Atomic Energy Commission and the National Aeronautics and Space Administration.

REFERENCES

1. D. E. Lea, Actions of Radiations on Living Cells, The Cambridge University Press, England, 1954.

2. G. Dolphin and F. Hutchinson, The Action of fast carbon and heavier ions on biological materials. Radiation Res. 13, 403-414 (1960).

3. N. Oda, Relationships between primary energy transfer and target theory. Presented at panel on "Biophysical Aspect of Radiation Quality," Vienna, April 1965, IAEA. (In press)

4. M. E. Rudd and T. Jorgensen, Jr., Energy and angular distribution of electrons ejected from hydrogen and helium gas by protons. Phys. Rev. 131, 666-675 (1963).

5. L. V. Spencer and V. Fano, Energy spectrum resulting from electron slowing down. Phys. Rev. 93, 1172-1181 (1954).

6. R. D. Birkhoff, H. H. Hubbell, Jr., J. S. Cheka, and R. H. Ritchie, Spectral distribution of electron flux in a beta-radioactive medium. Health Phys. 1, 27-33 (1958).

7. E. J. Sternglass, Backscattering of kilovolt electrons from solids. Phys. Rev. 95, 345-358 (1954).

8. J. E. Holliday and E. J. Sternglass, Backscattering of 5-20 keV electrons from insulators and metals. J. Appl. Phys. 28, 1189-1193 (1957).

9. H. Kanter, Electron scattering by thin foils for energies below 10 keV. Phys. Rev. 121, 461-471 (1961).

10. L. V. Spencer, Energy Dissipation by Fast Electrons, NBS Monograph 1, U. S. Department of Commerce, Washington, D. C., 1959.

11. For a review on the "track" model, see J. L. Magee, Ann. Rev. Phys. Chem. 12, 389-410 (1961); E. J. Hart and R. L. Platzman, in Mechanisms in Radiobiology (M. Errera and A. Forssberg, eds.), Vol. I, Chap. 2, Academic Press, New York, 1961.

12. A. Kupperman, Diffusion kinetics in radiation chemistry, in The Chemical and Biological Action of Radiations (M. Haissinsky, ed.), Vol. 5, pp. 85-166, Academic Press, New York, 1961.

13. R. E. Zirkle and C. A. Tobias, Effects of ploidy and linear energy transfer on radiobiological survival curves. Arch. Biochem. Biophys. 47, 282-306 (1953).

14. F. Hutchinson, The interaction of primary cosmic rays with matter and tissue, in Medical and Biological Aspects of the Energies of Space (P. A. Campbell, ed.), Columbia University Press, New York and London, 1961.

15. R. A. Shatas, J. F. Marshall, and M. A. Pomerantz, Dependence of secondary electron emission upon angle of incidence of 1.3-MeV primaries. Phys. Rev. 102, 682-686 (1956).

16. A. A. Schultz and M. A. Pomerantz, Secondary electron emission produced by relativistic primary electrons. Phys. Rev. 130, 2135-2141 (1963).

17. L. C. Northcliffe, Energy loss and effective charge of heavy ions in aluminum. Phys. Rev. 120, 1744-1757 (1960).

18. P. G. Roll and F. E. Steigert, Energy loss of heavy ions in nickel, oxygen, and nuclear emulsion. Nucl. Phys. 17, 54-66 (1960).

19. A. C. G. Mitchell and M. W. Zemansky, Resonance Radiation and Excited Atom, 2d ed, Cambridge Univ. Press, London, 1961.

20. H. S. Massey and E. H. S. Burhop, Electronic and Ionic Impact Phenomena, p. 145, Oxford University Press, London, 1952.

21. A. Kuppermann, Basic Mechanism in the Radiation Chemistry of Aqueous Media. In Radiation Res. Supplement 4, 15 (1964).

22. T. Hadeishi, O. A. McHarris, and W. A. Nierenberg, Radio-frequency resonance of the metastable state $(2^2P_{3/2}3^2\ S_{1/2})^2$ of neon produced and aligned by electron impact. Phys. Rev. 138, A983-A986 (1965).

23. R. L. Platzman, Superexcited States of Molecules, Radiation Res. 17, 419-425 (1962).

24. R. L. Platzman, Subexcitation electrons. Radiation Res. 2, 1-7 (1955).

25. R. L. Platzman, Total ionization in gases by high-energy particles. Intern. J. Appl. Rad. Isotopes 10, 116-127 (1961).

26. J. R. Greening, A contribution to theory of ionization chamber measurements at low pressure. Brit. J. Radiol. 27, 163-170 (1954).

27. E. Newman and F. E. Steigert, Response of NaI(Tl) to energetic heavy ions. Phys. Rev. 118, 1575-1578 (1960).

28. E. Newman, A. M. Smith, and F. E. Steigert, Fluorescent response of scintillation crystals to heavy ions. Phys. Rev. 122, 1520-1524 (1961).

29. A. Meyer and R. B. Murray, Effect of energetic secondary electrons on the scintillation process in alkali halide crystals. Phys. Rev. 128, 98-105 (1962).

FIGURE LEGENDS

Fig. 1. Schematic diagram of the experimental apparatus.

Fig. 2. Schematic diagram of the measuring circuit.

Fig. 3. Differential energy spectrum, assuming an isotropic angular distribution, for secondary electrons from an Al foil bombarded with He^4 ions.

Fig. 4. Differential energy spectrum, assuming a cosine angular distribution, for secondary electrons from an al foil bombarded with He^4 ions.

Fig. 5. Total absolute yield of secondary electrons with energies below 45 eV from a Ni foil as a function of Z^2_{eff} for 8.5-MeV/amu He^4, C^{12}, O^{16}, and Ne^{20} ions and for 8.8-MeV/amu O^{16} ions.

Fig. 6. Total yield of secondary electrons with energies below 45 eV from a Ni foil as a function of dE/dx for heavy ions with different velocities.

Fig. 7. Specific fluorescence of a NaI(Tl) crystal as a function of dE/dx (redrawn from reference 27).

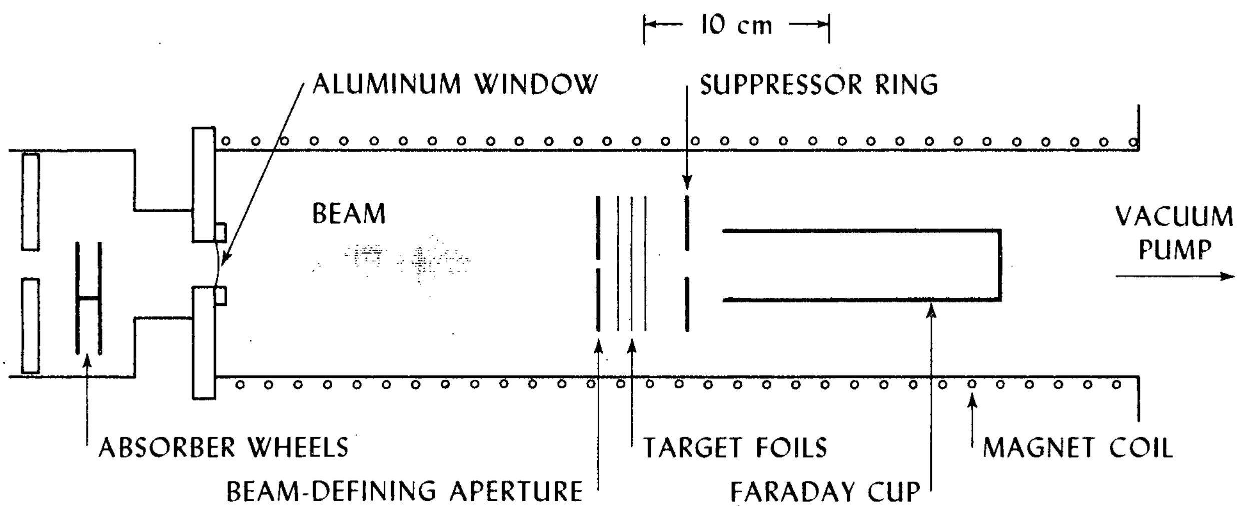

MUB-8229

Fig. 1

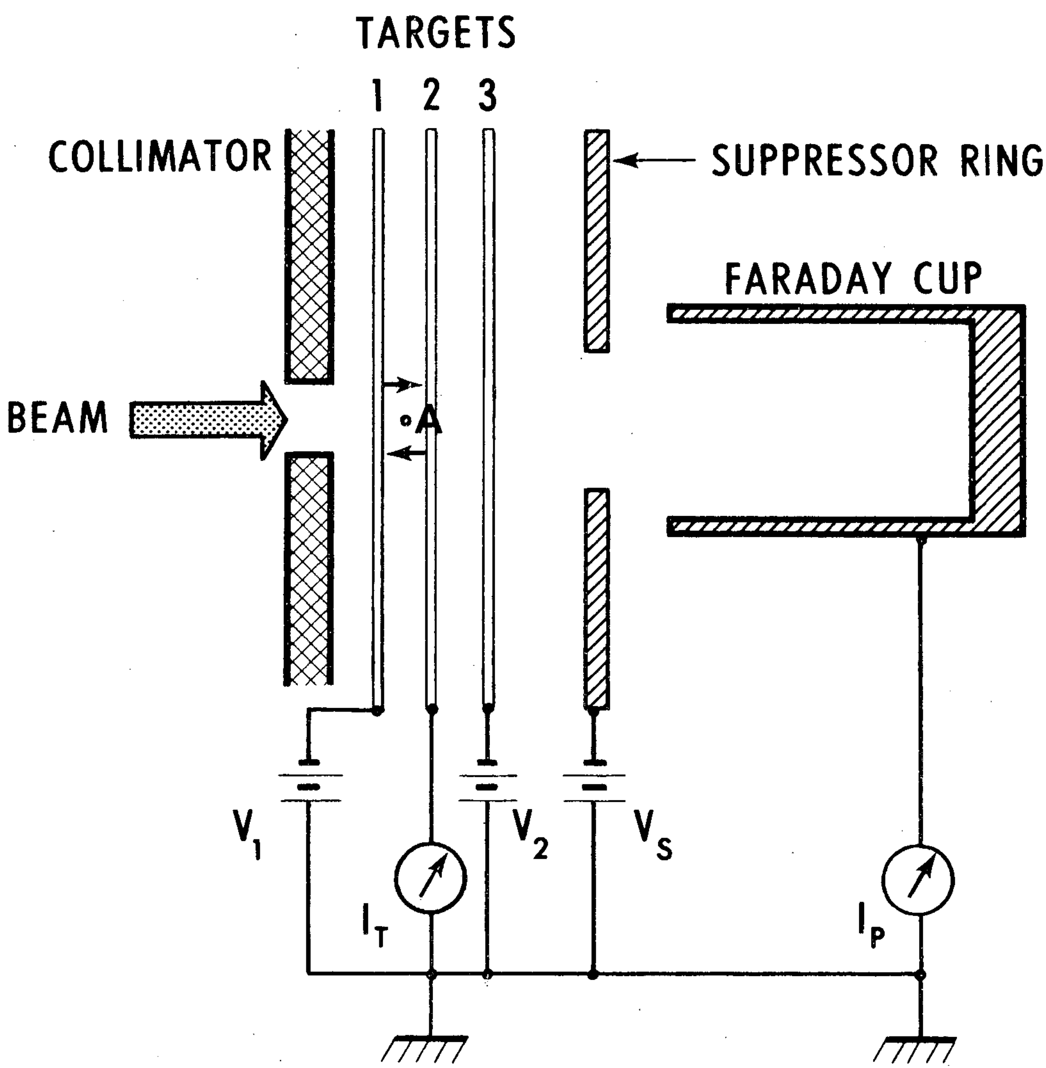

MUB-12645

Fig. 2

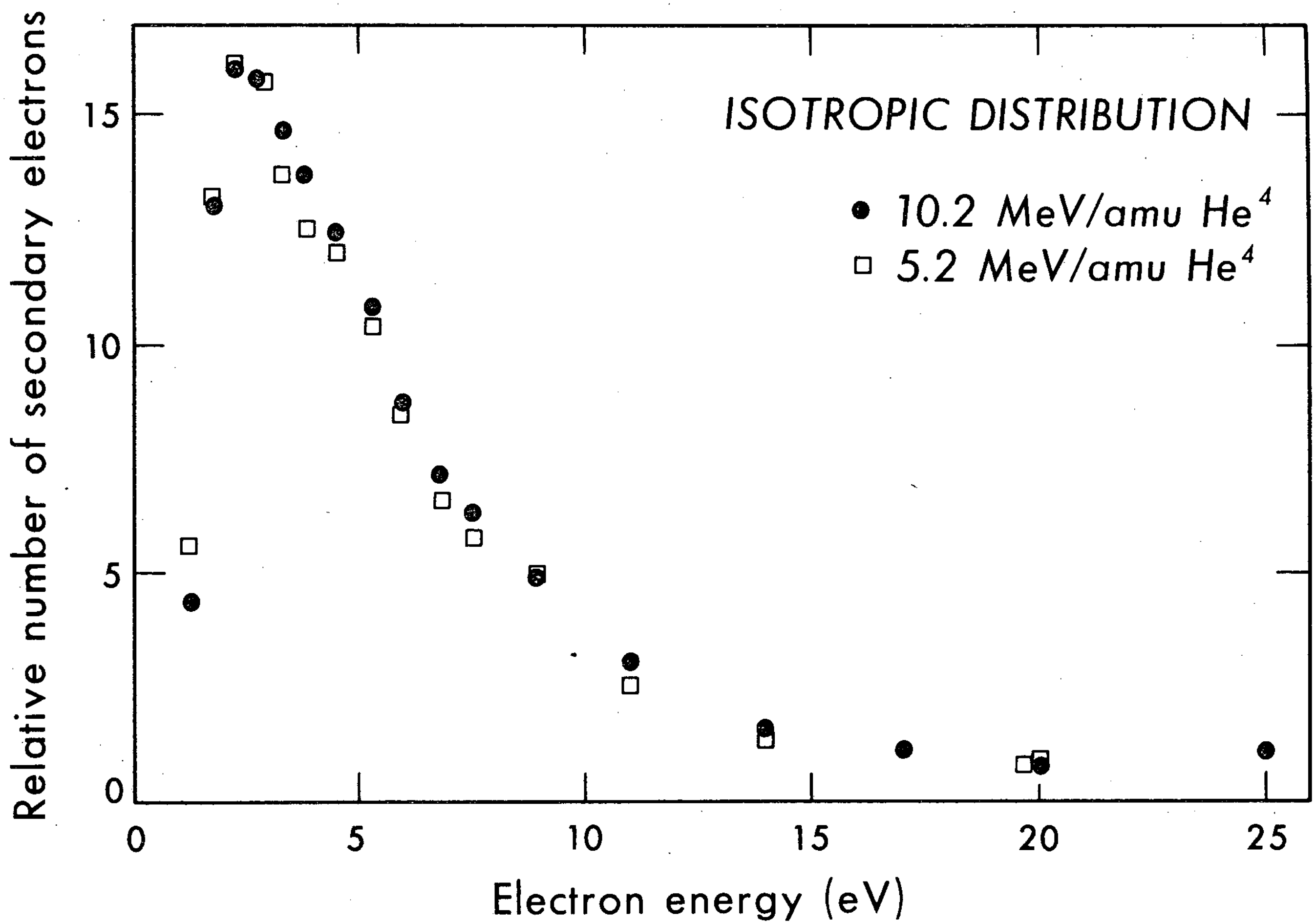

MUB-8230

Fig. 3

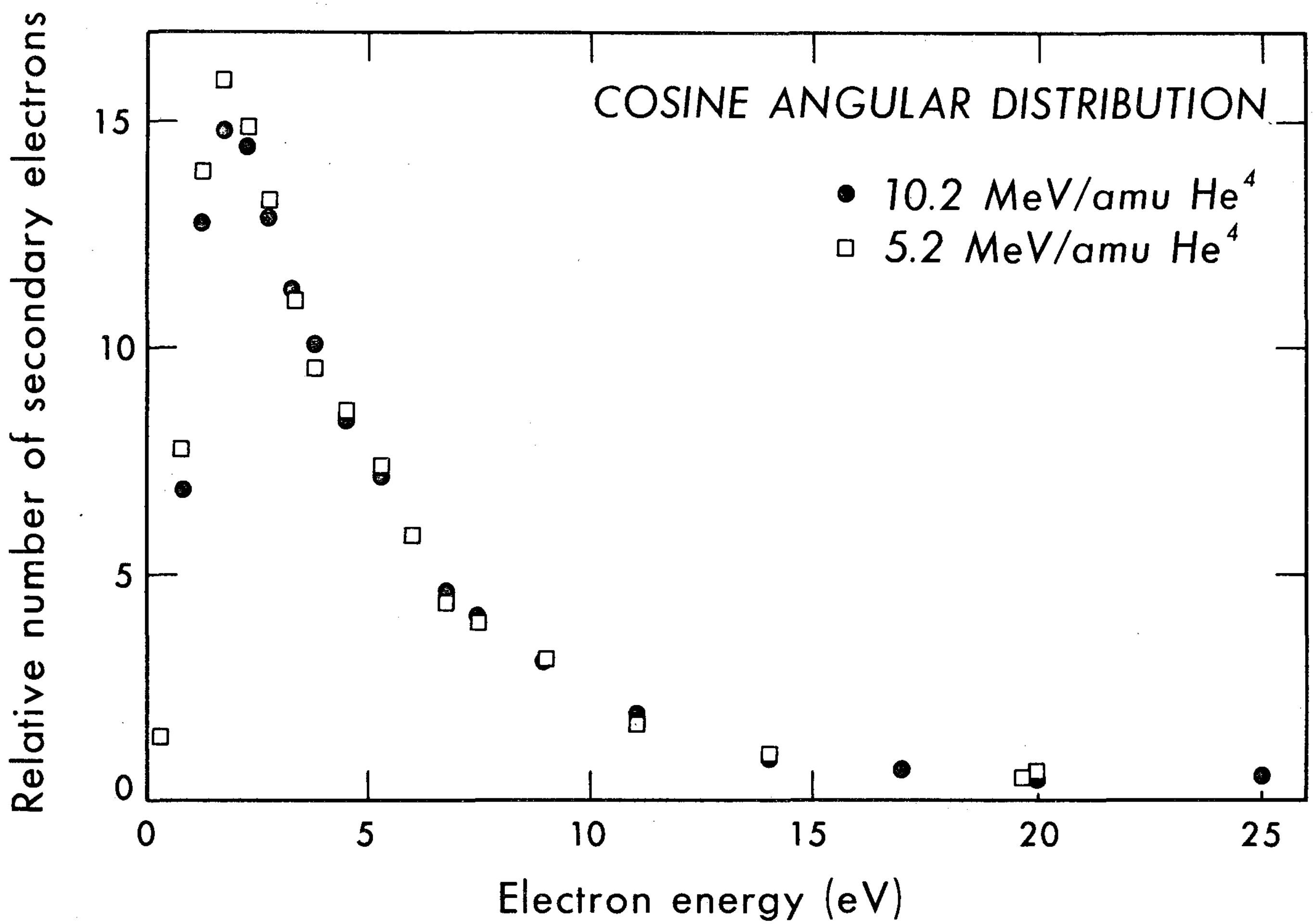

MUB-8231

Fig. 4

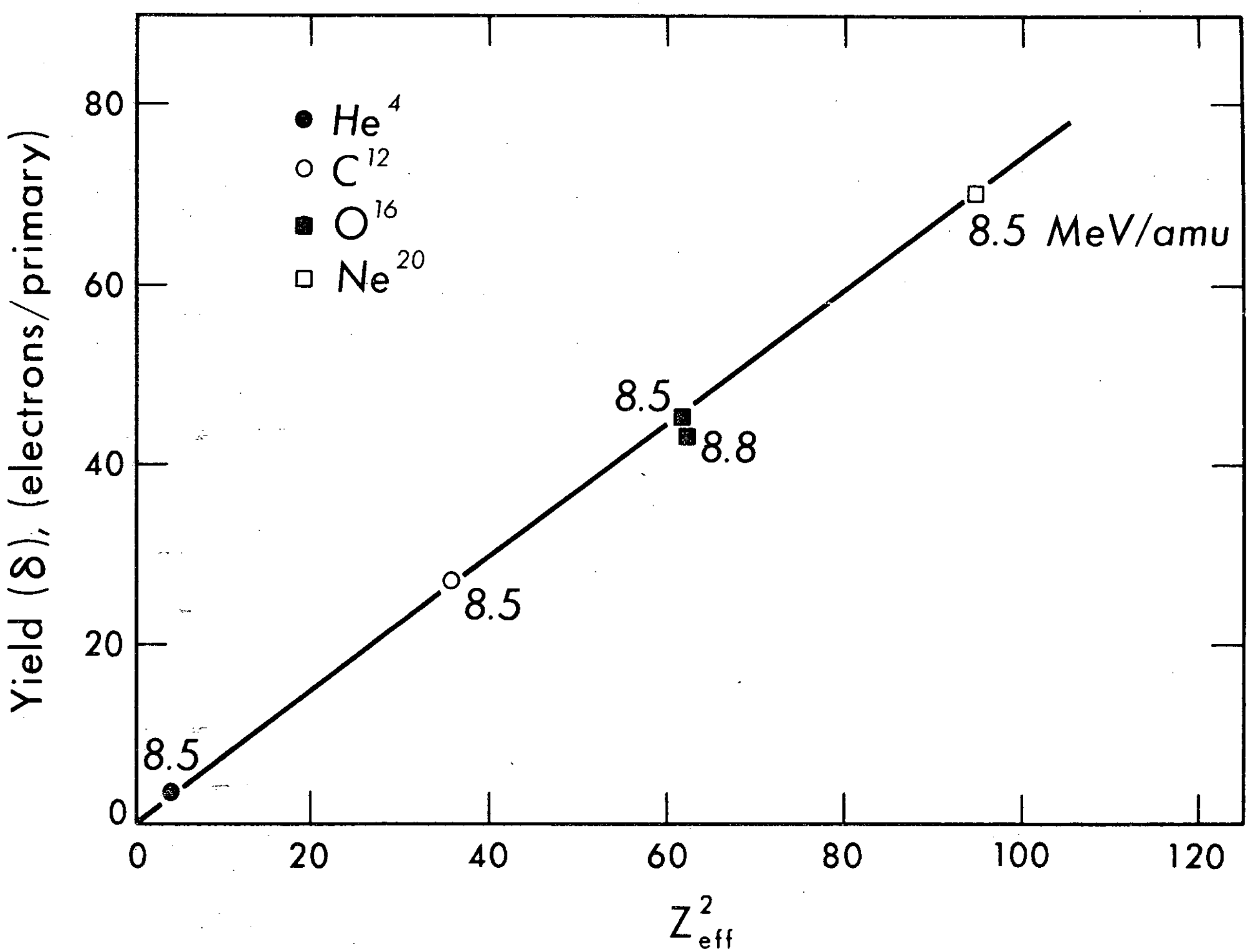

MUB-8232

Fig. 5

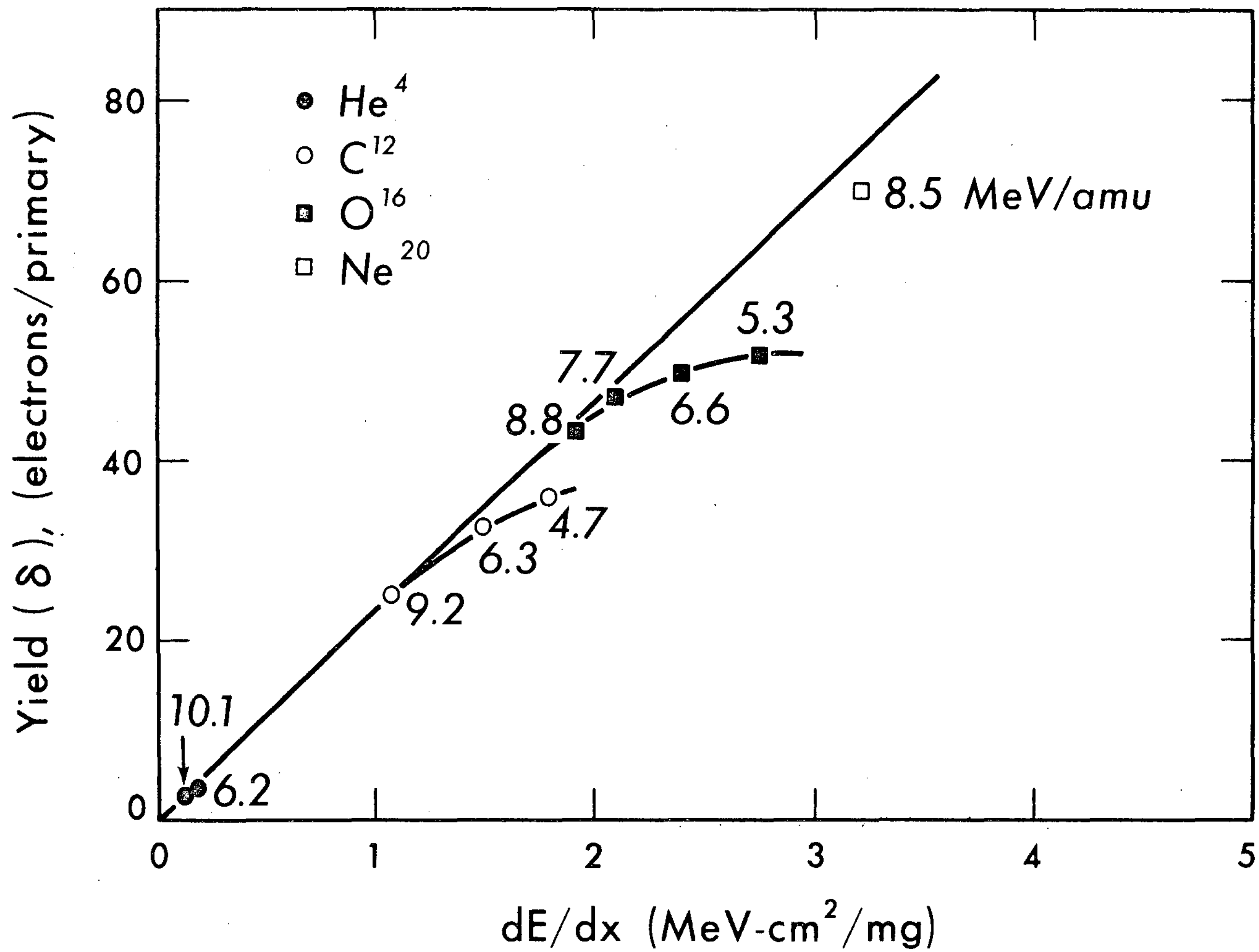

MUB-8233

Fig. 6

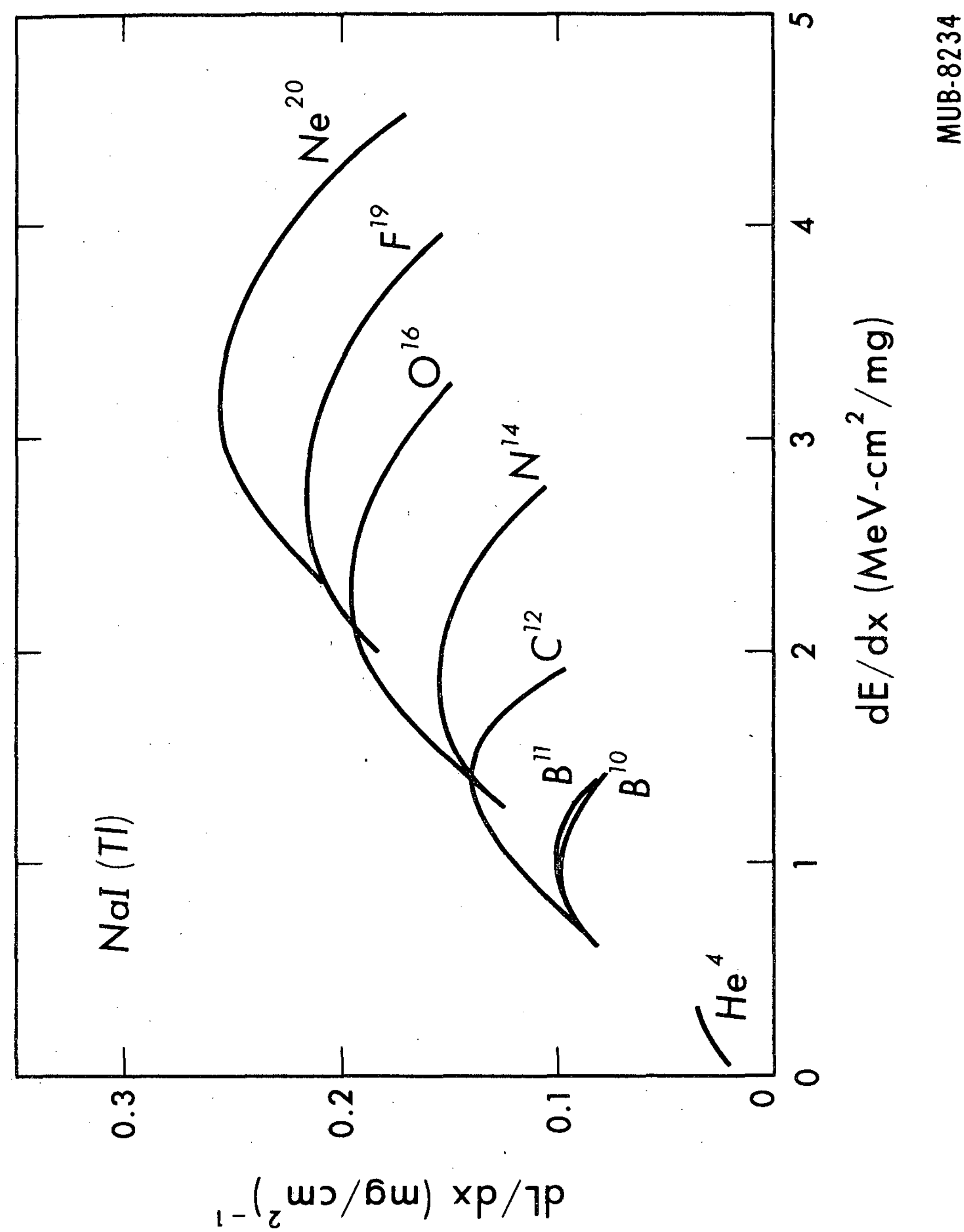
NaI (Tl)
He^4
B^10
B^11
C^12
N^14
O^16
F^19
Ne^20
0
0.1
0.2
0.3
dL/dx (mg/cm^2)^-1
0
1
2
3
4
5
dE/dx (MeV-cm^2/mg)
MUB-8234

Fig. 7